Nano Research

ISSN 1998-0124 CN 11-5974/O4
https://doi.org/10.1007/s12274-022-4466-4

Research Article

Perovskite quantum dot microarrays: *In situ* fabrication via direct print photopolymerization

Xiu Liu[1,§], Jianjun Li[1,§], Pingping Zhang[2], Weitong Lu[2], Gaoling Yang[1,3] (✉), Haizheng Zhong[2], and Yuejin Zhao[1] (✉)

[1] *School of Optics and Photonics, Beijing Institute of Technology, Beijing 100081, China*
[2] *MIIT Key Laboratory for Low Dimensional Quantum Structure and Devices, School of Materials Sciences & Engineering, Beijing Institute of Technology, Beijing 100081, China*
[3] *MIIT Key Laboratory for Low Dimensional Quantum Structure and Devices, Beijing 100081, China*
[§] *Xiu Liu and Jianjun Li contributed equally to this work.*

Received: 8 March 2022 / **Revised:** 16 April 2022 / **Accepted:** 21 April 2022

ABSTRACT

Quantum dots color conversion (QDCC) is considered as a facial and versatile way to achieve full-color organic light emitting diode (OLED) and micro-LED display due to the wide color gamut performance and easy integration. However, the aggregation of QDs and coffee-ring effects after solvent evaporation lowers the light conversion efficiency and emission uniformity in QDs microarrays, raising blue-light leakage or optical crosstalk. Here, we report the fabrication of perovskite quantum dots (PQDs) microarrays by combining the inkjet printing and *in situ* fabrication of PQDs during the photopolymerization of precursor ink. The resulting PQDs microarrays exhibit three-dimensional (3D) morphology with hemisphere shape as well as strong photoluminescence, which is desirable for QDCC applications. We demonstrate the dominant role of ultraviolet (UV) curable precursors and surface functionalized substrate in controlling the shape of microarrays, where significantly increased contact angle (100°) and large height to diameter ratio (0.42) can be achieved. We further demonstrate the potential use of the *in situ* direct print photopolymerization method for fabricating large-area multicolor patterned pixel microarrays with a wide color gamut and high resolution. The fabrication of 3D PQDs microarrays opens up new opportunities in a variety of applications including photonics integration, micro-LED, and near-field display.

KEYWORDS

quantum dots, perovskite, *in situ* fabrication, inkjet printing, microarrays

1 Introduction

Quantum dots color conversion (QDCC) has become a foundational technology for the design of full-color light-emitting devices with dramatically improved color performance, including organic light emitting diode (OLED) and micro-LED [1–3]. However, conventional and recently reported QDCC pixels fabricated by most commonly used inkjet printing of quantum dots (QDs) solution are still too thin to achieve efficient color conversion from excitation light sources, raising blue-light leakage or optical crosstalk [4]. Recently, perovskite QDs (PQDs) are emerging as attractive materials to maximize the color conversion efficiency by their superior optical properties and extremely large absorbance coefficient, kind of resolve this problem in terms of materials, but still not enough [5–9]. From a structure perspective, patterned black photoresist molds were manufactured to mold the QDs pixels, which has a certain effect in increasing the pixel thickness and avoiding the optical crosstalk, but the manufacturing cost will increase substantially [2, 10–12]. Thus, development of an improved method by combing powerful absorbed PQDs with highly structured pixel morphology (for example, three-dimensional (3D) structure) is highly desirable for next-generation displays [13, 14].

Inkjet printing, a widely used deposition method for inorganic and organic optoelectronics, has attracted great attention in patterned microarrays by its non-contact, material-efficient, and reproducible processing [15–17]. Using this method, colloidal QDs can be deposited directly onto the substrate to form pixelated microarrays with multi-color, bright luminescence, and high resolution for display application [18–23]. In particular, *in situ* fabricated PQDs have recently emerged as promising optimal ink for inkjet printing [24–27]. The low formation enthalpy and high defect tolerance of perovskite allow for the *in situ* fabrication of high-quality PQDs directly on a substrate or in a matrix including polymer [28], glass [29], crystals [30], fibers [31], or printed droplets [25], wherein patterned PQDs microarrays can be formed by printing the perovskite precursor ink on the substrate then *in situ* crystallization. The *in situ* inkjet printed PQDs microarrays show improved stability and photoluminescence (PL) strength over the pre-prepared PQDs inks, which usually suffer from their fragile surface chemistry and aggregation problems during the long-term storage and printing process [32–34]. However, the color conversion applications of these *in situ* printed PQDs microarrays are still limited by their thin thickness therefore an inadequate absorption of ultraviolet (UV)/blue light, and their poor surface morphology uniformity which is usually caused by the intrinsic coffee-ring effect during the inkjet printing

Address correspondence to Gaoling Yang, glyang@bit.edu.cn; Yuejin Zhao, yjzhao@bit.edu.cn

process [35, 36]. Nevertheless, the construction of *in situ* fabricated PQDs microarrays with high light conversion efficiency and emission uniformity remains a challenge.

As a macromolecular synthesis methodology, polymerization can manufacture various complex structured materials with high efficiency and controllability, which show increasing promise for various applications including coatings, inks, optoelectronics, laser imaging, advanced manufacturing, and biomedical engineering [37–40]. Recently, photopolymerization was utilized to provide a robust and flexible host matrix for QDs patterns with 3D structure [10, 41–43]. However, the incompatibility between QDs and polymers will result in the aggregation of QDs and further high optical scattering and losses. Inspired by these achievements, here we present an *in situ* direct print photopolymerization method to fabricate PQDs microarrays by combining the inkjet printing and *in situ* fabrication of PQDs during the photopolymerization of precursor ink. The resulting PQDs microarrays exhibit the excellent PL property of *in situ* fabricated PQDs as well as 3D hemispherical morphology, desirable for QDCC applications. More notably, the dominant role of UV curable precursors and surface engineering on substrates for the shaping of microarrays was discovered, where a significantly advanced contact angle (100°) and a large height to diameter ratio (0.42) with height up to 17 μm can be achieved. Moreover, PQDs microarrays exhibited blue, green, red, and mixing fluorescence with wide color gamut, large-area, and high-resolution were demonstrated by controlling the halogen ions in precursor inks.

2 Experimental

2.1 Chemicals and materials

Lead chloride ($PbCl_2$, 99.9%), lead bromide ($PbBr_2$, 99.9%), lead idodide (PbI_2, 99.9%), methylamine hydrochloride (CH_3NH_3Cl, 98%), methylamine hydrobromide (CH_3NH_3Br, 98%), Cesium iodide (CsI, 99.9%), and dimethyl sulfoxide (DMSO) were purchased from Aladdin Reagent. 2-Phenylethanamine bromide (PEABr, > 99.5%) was purchased from Xi'an Polymer Light Technology Corp. Polyacrylonitrile (average M_W 150,000) was purchased from Innochem, polyvinylidene fluoride (average M_W 400,000) was purchased from Arkema, and the UV-curing acrylic resin was provided by Hangaoda. All reagents were used without further purification.

2.2 Preparation of inkjet printing inks

Green perovskite precursor ink was fabricated by dissolving CH_3NH_3Br (0.037 g, 0.3 mmol), $PbBr_2$ (0.057 g, 0.15 mmol), and 0.02 g UV curing resin into DMSO solution (1 mL, 14.10 mmol). Blue perovskite precursor ink was made by dissolving CH_3NH_3Cl (0.027 g, 0.4 mmol), PEABr (0.0734 g, 0.36 mmol), $PbBr_2$ (0.0734 g, 0.2 mmol), and 0.02 g UV curing resin into DMSO solution (1 mL, 14.10 mmol). Red perovskite precursor ink was made by dissolving CsI (0.0338 g, 0.13 mmol), PbI_2 (0.03 g, 0.065 mmol), $PbBr_2$ (0.023 g, 0.062 mmol), and 0.02 g UV curing resin into DMSO solution (1 mL, 14.10 mmol).

2.3 Fabrication of PQDs microarrays

ITO substrate was first cleaned by ultrasonication successively in acetone, deionized water, and isopropyl alcohol, after being dried by using flowing nitrogen gas, the PDMS/UV curing resin was spin-coated on the blank substrate at a spinning rate of 2,000 rpm for 45 s and then heat at 120 °C for 30 min. The inkjet printing on the polymer-modified substrate was accomplished by using a Sonoplot printer equipped with a 30 μm diameter piezoelectric driven inkjet nozzle. After printing, the precursor droplets were fully cured by illuminating 30 s with a 365 nm handheld UV lamp at a power of 5 W to model microarrays. After curing molding, the substrate with perovskite precursor microarrays was heated at 40–80 °C for 10–30 min to complete *in situ* crystallization of PQDs. All printing, curing, and annealing were done in ambient conditions.

2.4 Materials characterizations

The static contact angles were measured on a contact-angle system (SL150E, USA KINO Industry Co., Ltd) with latex droplets (2 μL). The morphologies were observed by scanning electron microscopy (SEM) (Hitachi, Model S-4800). Cross-sectional transmission electron microscopy (TEM) image was analyzed using a JEM 2100F (JEOL) operating at 200 kV, while the ultrathin section was prepared using Leica EM UC7 ultramicrotome. The heights of microarrays were measured by step profiler (Dektak XT, Bruker). The PL spectra were measured with a fluorescence spectrophotometer (SpectraScan, PR-655) with an excitation wavelength of 365 nm. The fluorescence microscope images of microarrays were obtained using a laser scanning confocal microscope (Nikon, N-SIM A1R).

3 Results and discussion

The fabrication process of PQDs microarrays via *in situ* direct print photopolymerization technique is illustrated in Fig. 1. Prior to inkjet printing, PDMS mixed with curing agent was spin-coated onto the quartz glass substrate, pre-curing for about 30 min at 120 °C to form a solid hydrophobic polymer film. Such surface modification is critical for the successful inkjet printing of microarrays. After that, the inkjet printing process was conducted by continuously ejecting the perovskite precursor ink droplets onto the modified substrate from a piezoelectric nozzle. The precursor ink was obtained by mixing methylamine hydrobromide (MABr), lead bromide ($PbBr_2$), and UV curing resin in DMSO (see Fig. S1 in the Electronic Supplementary Material (ESM) and Experimental section). Each droplet can form an individual pixel after being completely cured, the size of these microarrays can be controlled by adjusting the printing parameters including printing distance, release voltage, and time, as well as the size of the nozzle. Once the droplet reached the PDMS substrate, a spherical cap will shape immediately, with the perovskite precursor and UV curing resin randomly distributed. After the patterned microarrays were fabricated by continuous inkjet printing, UV light was irradiated to the substrate, curing the fluid convex and forming regular microarrays patterns. Subsequently, with the removal of residual DMSO in the droplet at a certain temperature, the concentration of $MAPbBr_3$ reaches its critical value and then nucleation, PQDs microarrays were formed.

Figures 1(b) and 1(c) show the corresponding SEM images of the PQDs microarrays, demonstrating their great size homogeneity and conforming their 3D dome-shaped patterns, thanks to the well-controlled droplet shape in the printing process. In addition, cross-sectional TEM measurement was performed to clearly demonstrate the QD structure of *in situ* crystallized $MAPbBr_3$ perovskites, as shown in Fig. S2 in the ESM. Figure 1(d) shows the fluorescence image of PQDs microarrays under laser scanning confocal microscope, the printed microarrays emit bright and uniform green fluorescence under UV irradiation. The fluorescence image of an individual PQDs microarray was further enlarged (Fig. S3 in the ESM), from which we can see more clearly that the brightness in the center and the edge is almost the same as in other sections, demonstrating the highly uniform distribution of PQDs in these microarrays where normally coffee ring effect is missing.

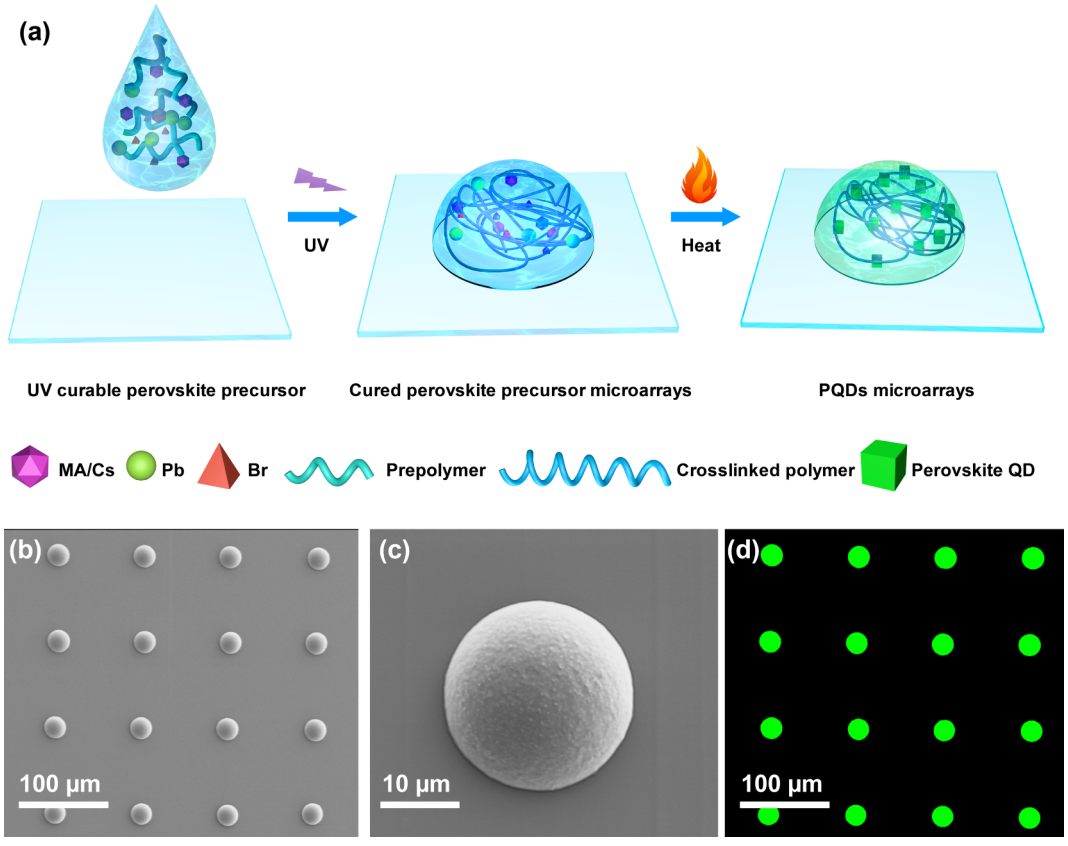

Figure 1 *In situ* direct print photopolymerization fabrication of PQDs microarrays. (a) Schematic showing the fabrication of PQDs microarrays through *in situ* direct print photopolymerization method. (b) SEM image of the resulting PQDs microarrays. (c) SEM image of an individual PQDs microarray. (d) Fluorescence microscope image of green $MAPbBr_3$ PQDs microarrays.

There are two crucial factors that make PQDs microarrays possible: the UV curable perovskite precursors and surface functionalization of the printing substrate. To achieve our goal of printing PQDs microarrays with regular hemispherical shapes, a seemingly straightforward but challenging approach is to generate an appropriate droplet on the substrate. Therefore, we first try to control the morphology of droplets by adjusting the viscosity, density, and surface tension of the ink by adding a small amount of polymer, which is commonly used for patterned QDs pixels [25, 44–46]. However, with the evaporation of excess solvent that is used to dissolve polymers, the three-phase contact line continually slides along the smooth substrate surface, causing the spread of droplets over a large area and distorting the convex morphology of the droplets (see Fig. S4 in the ESM). Compared with the most used polymer additive such as polyvinyl pyrrolidone (PVP) or polyvinyl alcohol (PVA), UV curing resin is much more soluble in the matrix solution for PQDs precursor inks such as N,N-dimethylformamide (DMF) and DMSO. That means we can get suitable printing inks at a lower solvent ratio, which is extremely useful for reducing the solute movement rate and eliminating the coffee ring effect. What is more, an important advantage of direct printing of this curable perovskite precursor over other QDs inks is the light-curing property, which enables shape of the microarrays morphology more easily under UV light irradiation and is important for color conversion application.

To obtain high-quality PQDs microarrays, the printable of inks is a quite crucial issue for inkjet printing technique, which can be evaluated by the inverse Ohnesorge number Z (the ratio of surface tension and inertial forces to viscous forces)

$$Z = \frac{\sqrt{\gamma\rho\alpha}}{\mu}$$

where γ, ρ, and μ are the surface tension, density, and viscosity of the ink, respectively, and α is the diameter of the nozzle. As a matter of experience, the range of Z between 1 and 10 means good jetting. If the Z value is too small, there will be elongated tailing during printing or no droplets can be formed at all, while too large Z is usually accompanied by unwanted satellite droplets. The curing perovskite precursor ink shows a surface tension of 36.1 $mN{\cdot}m^{-1}$, a density of 1.18 $g{\cdot}cm^{-3}$, and a viscosity of 5.31 mPa·s. The calculated Z value is 5.50 when an inkjet nozzle with a diameter of 20 μm is used, demonstrating the suitability of the perovskite precursor ink for inkjet printing. What is more, the prepared UV curable perovskite precursors ink exhibits high stability, which can be stored for more than several months under ambient conditions (Fig. S1 in the ESM).

In addition to the precursor ink, substrate modification is another crucial factor in the shaping of microarrays. To further demonstrate the requisite of surface modification in regulating the contact angle and final morphology of microarrays, substrates either with any functional groups modified or the crude ones were tested and the results are summarized in Fig. 2(c). Evidently, compared with bare glass or silicon (Fig. S5 in the ESM), the polymer-modified substrate surfaces exhibited remarkably increased contact angles (60° for polyvinylidene fluoride PVDF as shown in Fig. 2(a), 70° for polyacrylonitrile PAN, and 90° for PDMS, Fig. S6 in the ESM), demonstrating that polymer coating can impact the hydrophilic nature of substrates. The hydrophobicity of these polymer-modified substrates resulted in the depinning of the three-phase contact line of the droplets, preventing the formation of coffee rings and leading to two-dimensional (2D) hemisphere-shaped microarrays. The higher contact angles almost approach 90° for PDMS modified surfaces indicate the enhanced hydrophobicity behavior and lower surface energy, which may come from the bulkier alkyl groups [47]. In addition to the hydrophobic properties, the solvent resistance of

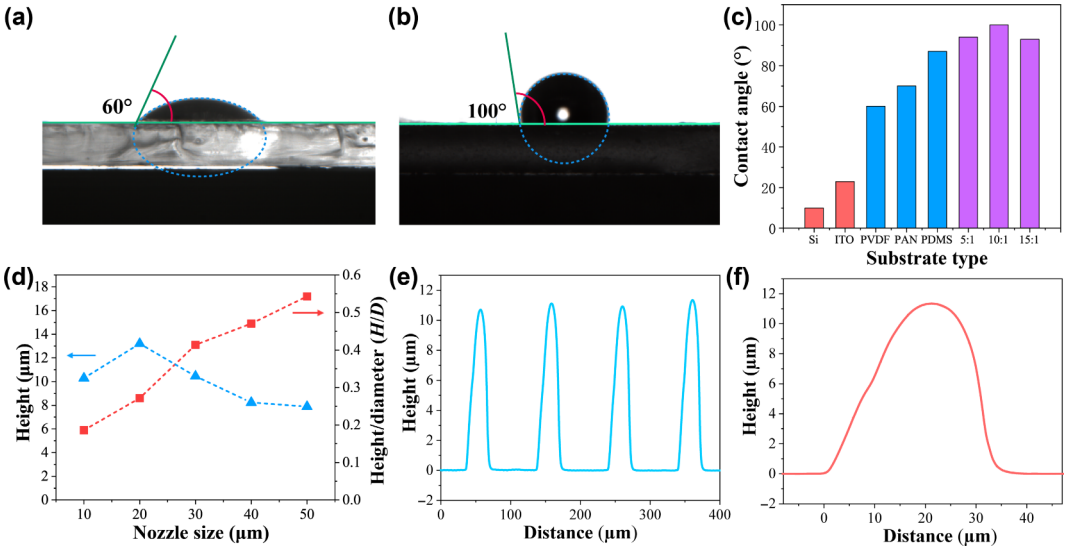

Figure 2 Morphology and size control of inkjet-printed PQDs microarrays. (a) Contact angles of UV curing resin on PVDF substrate. (b) Contact angles of UV curing resin on the substrate with 10:1 PDMS/curing agents. (c) The relationship between contact angle and substrate type. (d) The height and *H*/*D* of microarrays versus nozzle size. (e) Geometries of microarrays measured via step profiler. (f) The geometry of an individual PQDs microarray.

the used polymers is another key factor. Compared to PDMS, DMSO has the ability to dissolve PVDF and PAN, which will lead to smaller contact angles to some extent. To further increase the contact angle, different amounts of curing agents were added. The increased contact angle up to 100° can be explained by an enhanced hardness after UV curing (Fig. 2(b) and Fig. S6 in the ESM), and thus an increase of adhesion ability of the substrates to the three-phase contact line, leading to strong binding of droplets onto the substrate and lowing the solute movement rate [48].

To explore the parameters for the adjustment of diameter and height of microarrays, we printed microarrays under varying printing parameters, such as the printing distance, the release voltage, the release time, the nozzle size, and so forth (see Figs. S7 and S8 in the ESM). As an example, Fig. 2(d) shows the overall relationship between the height to diameter ratio (*H*/*D*) of microarrays and the nozzle size. The height of microarrays increased linearly as a function of the nozzle size, the average heights of the microarrays were 5.9, 8.6, 13.1, 14.9, and 17.2 μm, corresponding average diameters increase from 18.2 to 69.1 μm (Fig. S9 in the ESM), while the largest *H*/*D* can reach up to 0.42 when the nozzle diameter was fixed at 20 μm. To study the voltage effect on the formation of microarrays, different release voltages were used and the images of printed microarrays are shown in Fig. S7 in the ESM. Microarrays are only formed at a proper release voltage of less than 2 V, and higher voltage is unfavorable due to the uneven precursor inks output. For the release time, which is the duration time of continuous deposition of droplets when the releaser needle stays on the substrate, the optimized upper limit should be no larger than 500 ms, especially when large size nozzles were used. Otherwise, it will cause the droplets to flatten and collapse on the substrate due to excessive ink output, affecting the morphology of the microarrays. The images of printed microarrays with different release times from 0 to 1,000 ms and nozzle sizes from 20 to 50 μm are shown in Fig. S8 in the ESM. To further verify the uniformity of microarrays that were printed under these optimized parameters, a step profiler was used to measure their geometrical properties and the results are shown in Figs. 3(e) and 3(f). The microarrays show almost the same diameter (35 μm) and height (11 μm), verifying their uniformly and 3D hemisphere morphology.

In the case of the same blue light source excitation for example micro-LED backlight, the upper surface of the convex cap can excite more light than the planar and concave one. The least amount of light emitted from the concave cap is due to the fact that the micro-LED light source is similar to the Lambert type luminescence, and the light intensity is largest near the center of the light source while the surrounding light intensity is low. For a concave QDs cap, the middle thickness is thinner but the thickness around the periphery is larger, so the concave cap absorbs less blue light, most of the blue light passes through the QDs, and the corresponding emitted light is less. Although the center thickness of the convex cap is large and the surrounding thickness is small, it absorbs less blue light compared with the planar one, mainly due to the blue light at a certain angle on the upper planar surface will be fully reflected and reabsorbed, while the exciting light from the same angle in the convex cap can be transmitted from the upper surface. Due to the same reason, the planar cap emitted less light than the convex one as the emitted light is also reflected back and absorbed by the QDs. Overall, for planar, concave, and convex QDs caps with the same volume and the same concentration, the convex one can absorb more energy from the exciting blue light and reduce the total internal reflection of light as it passes through the upper surface, which is more suitable for the color conversion application.

As a usage-centered approach, large-scale production is essential. To demonstrate the promising advantage of our strategy for large-scale optical application, large-area $MAPbBr_3$ PQDs microarrays were printed and shown in Fig. 3 and Fig. S10 in the ESM. By carefully optimizing the driving voltage (1 V) and printing release time (500 ms) while using a small size nozzle (20 μm), large-scale high-resolution microarrays with a diameter of ≈ 30 μm and a height of ≈ 10 μm were demonstrated on centimeter-scale substrates, as shown in Fig. 3(a). Feature sizes on an order of 100 μm are necessary for most the practical applications, for example, 150 μm pixel size is enough for a 13″ full high-definition (HD) display, which means our microarrays match the present resolution requirement for display. To further punch up the high resolution of our microarrays, the pixels-per-inch of 21.5″ iMac 4K display is about 218 while the large-area printed microarrays are beyond 500, far exceeding the resolution of current display panels, not to mention higher-resolution microarrays can be achieved by using a smaller size nozzle, suggesting the fidelity of our QDs microarrays used as color conversion pixels. The enlarged fluorescent image and three-dimensional laser confocal microscope fluorescent image of the microarrays show a homogeneous and bright fluorescence on the

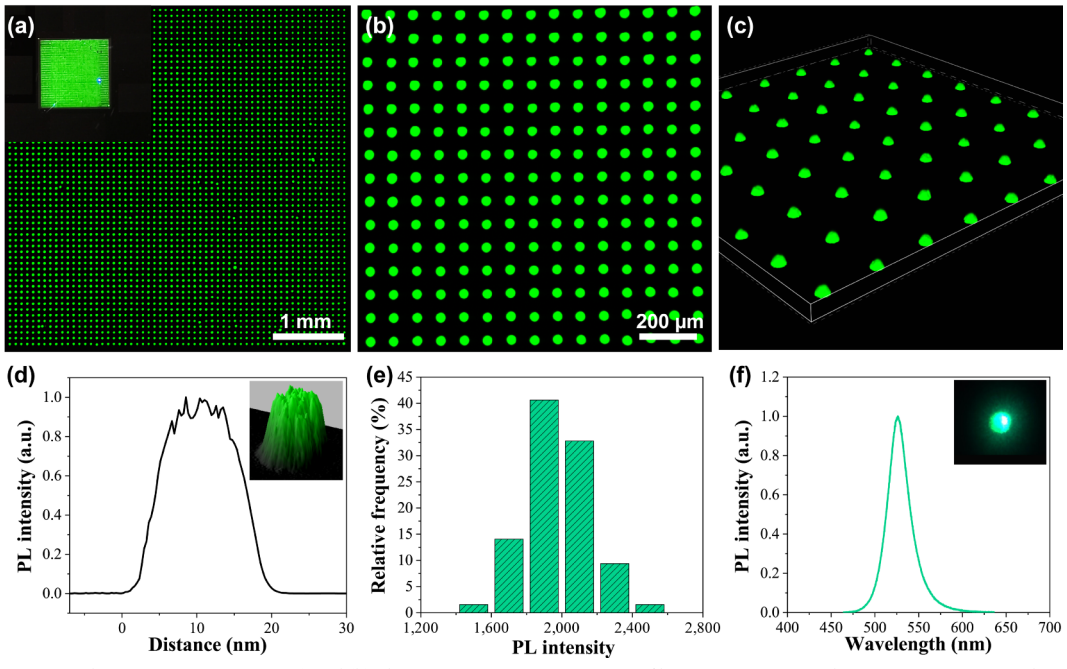

Figure 3 Large-area $MAPbBr_3$ PQDs microarrays. (a) and (b) Fluorescence microscope images of large-area green $MAPbBr_3$ PQDs microarrays showing the uniform size and a well-defined pattern. (c) Three-dimensional laser confocal microscope photograph of the PQDs microarrays. (d) PL intensity distribution of an individual QDs microarray. (e) Statistic graphics of PL intensity of the PQDs microarrays. (f) PL spectrum of an individual $MAPbBr_3$ PQDs microarray, while the inset is its optical image under a 405 nm laser illumination.

microscale, further demonstrating the excellent uniformity and reproducibility of every individual PQDs microarrays fabricated by the inkjet printing method (Figs. 3(b) and 3(c)). Figure 3(d) is the PL intensity distribution of a single pixel, indicating a positive relationship between the PL intensity and the height of the pixel. The top view and profile photographs of one pixel were observed under the 3D laser scanning confocal microscope and shown in Fig. S11 in the ESM, illustrating the uniformity of PL intensity. The PL intensity statistic graphics of the QDs microarrays are shown in Fig. 3(e). The narrow PL intensity distribution demonstrates the uniformity of the microarrays, as well as the homogeneous nucleation of PQDs in these microarrays. Figure 3(f) gives the PL spectrum of an individual $MAPbBr_3$ PQDs microarray illuminated using a beam of 405 nm wavelength laser, the microarrays show an intense green emission band centered at 526 nm with narrow full width at half maximum of 28 nm, while the inside real-color photograph further clearly shows a very uniform emission image. What is more, the PL spectrum remains constant after months, which indicates that the green-emitting $MAPbBr_3$ PQDs microarrays have good stability due to the use of UV curing resin, which is a critical parameter for color conversion micro-LED display application.

We further fabricated blue and red color emissive perovskite microarrays by varying the halides of precursor ink from Br to Cl or I [5]. Figures 4(a)–4(c) and Fig. S12 in the ESM show fluorescent images of the printed macroscopic letters BIT composed of blue, green, and red PQDs microarrays, which show a bright emission under 365 nm excitation. The detailed views of these microarrays are shown in Figs. 4(d)–4(f), we can see bright and homogeneous light emit from all these arrayed microarrays, confirming the realization of high quality regularly blue and red arranged microarrays, manifesting the excellent reliability of the *in situ* direct print photopolymerization method further. These fabricated microarrays exhibit a narrow fluorescence emission peak with maximum intensity at 472, 526, and 654 nm, respectively, as shown in Fig. 4(g). The PLQY for the printed red-, green-, and blue- PQD microarrays is 10%, 35%, and 20%, respectively, and more efforts are needed to optimize the precursor inks and printing parameters. Figure 4(h) is the color point of these trichromatic microarrays in the color Commission Internationale del'éclairage (CIE) 1931 color coordinate triangle, and the microarrays achieved a wide color gamut than wide-gamut high-definition television (HDTV) production, implying their outstanding full-color fluorescence properties for color conversion display applications. The color coordinates area of the microarrays is larger than that of the color space of the NTSC (≈ 112% of NTSC 1931) standard, much larger than that of HDTV (≈ 157% of HDTV) standard. Significantly, the color point of the green microarrays (0.19, 0.74) is much better than the green standard of the HDTV, even close to the green standard Recommendation Rec. 2020 (0.17, 0.79), which can help promote the display colors visually since human eyes are more sensitive to the green tones [3]. What is more, the blue microarrays showed an emission peak at 472 nm and narrow full width at half maximum less than 30 nm, which is more suitable as health blue light in the display. To further extend the application of the PQDs microarrays, multicolor arrays were realized based on the *in situ* direct print photopolymerization method. Figure 4(i) shows pixel arrays with red and green microarrays, and a full-color display can be achieved after combining these double color conversion pixels with blue micro-LED chips. This combination not only provides red LED chips but also reduces the immature mass-transfer process, significantly decreasing the power and cost consumption. The above results further confirm the realization of high-quality multicolor microarrays through the inject printing approach, paving the way for the further fabrication of full-color QDCC micro-LED display.

4 Conclusions

In summary, PQDs microarrays with 3D hemisphere morphology and strong PL are fabricated by *in situ* direct print photopolymerization strategy. High contact angle up to ~ 100° and large height to diameter ratio approach 0.42 are demonstrated by adjusting the printing parameters and substrates. We found that UV curable perovskite precursors and surface functionalization of the printing substrate are two crucial factors that make PQDs microarrays possible. More importantly, these

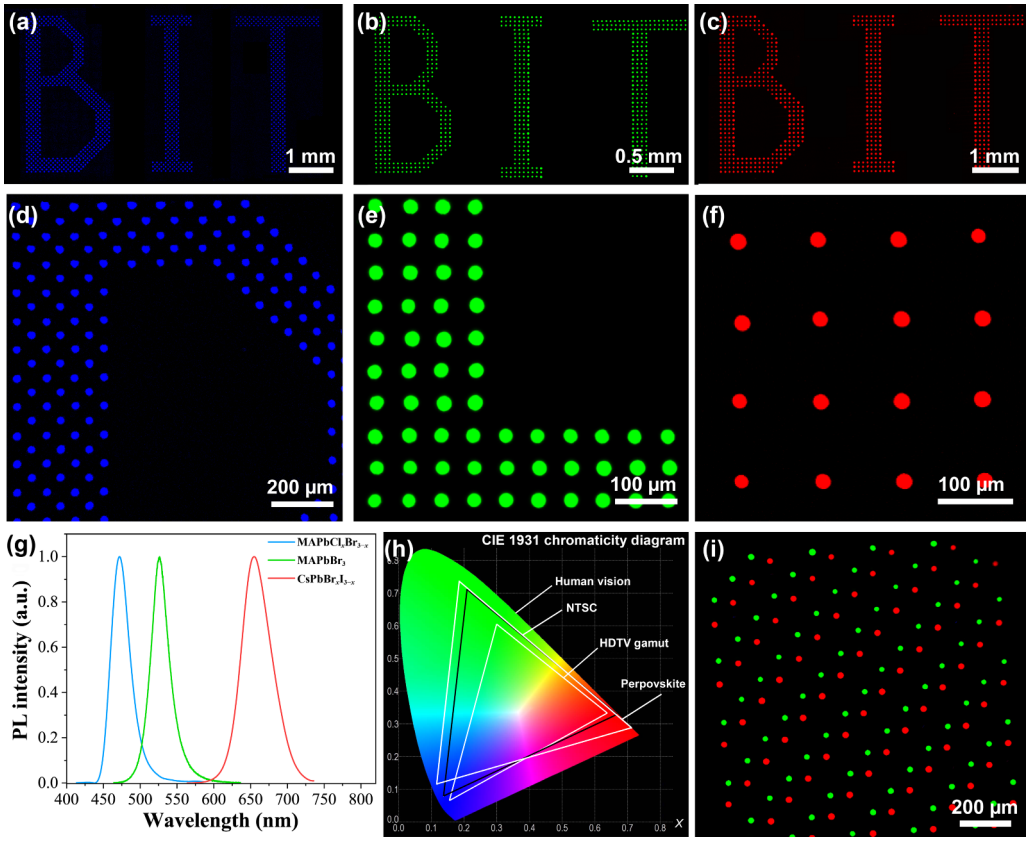

Figure 4 RGB full colored PQDs microarrays. Fluorescence images of macroscopic letters BIT composed of (a) blue ($MAPbCl_xBr_{3-x}$), (b) green ($MAPbBr_3$), and (c) red ($CsPbBr_xI_{3-x}$) emissive PQDs microarrays, and (d)–(f) their local enlarged images taken by confocal microscope. (g) Fluorescence spectra of blue, green, and red emission perovskite microarrays excited at 375 nm. (h) The color coordinates of blue, green, and red emission PQDs microarrays in the 1931 CIE chromaticity diagram along with standard NTSC and HDTV color space. (i) Fluorescence image of RG PQDs microarrays.

microarrays achieve strong and uniform PL in large-area due to their seamless integration with *in situ* fabricated PQDs. We further demonstrate the potential use of the *in situ* direct print photopolymerization method for fabricating patterned multicolor PQDs microarrays with a wide color gamut and high resolution. Therefore, compared with previous printing methods, this *in situ* direct print photopolymerization technique allows to precisely control the pixel structure, removing the aggregation of QDs and coffee-ring effects in microarrays, which will aid in their expansion in photonics integration, full-color display, on-chip biomedical diagnostics, and next-generation AR/VR devices.

Acknowledgements

This work was financially supported by the National Key Research and Development Program of China (No. 2020YFB2009303), the National Natural Science Foundation of China (Nos. 62105025 and 61935001), and Beijing Institute of Technology Research Fund Program for Young Scholars (No. 3040011182113). The authors would like to acknowledge the Experimental Center of Advanced Materials of Beijing Institute of Technology for the support in materials synthesis and characterization. We also acknowledge Prof. Ruibin Liu, Mr. Weifeng Ma, and Dr. Shuangyang Zou for the help in fluorescence spectra measurement.

Electronic Supplementary Material: Supplementary material (cross-section TEM measurements, contact angles, CCD images and 3D laser confocal microscope photograph) is available in the online version of this article at https://doi.org/10.1007/s12274-022-4466-4.

References

[1] Jang, E.; Jun, S.; Jang, H.; Lim, J.; Kim, B.; Kim, Y. White-light-emitting diodes with quantum dot color converters for display backlights. *Adv. Mater.* **2010**, *22*, 3076–3080.

[2] Hu, Z. P.; Yin, Y. M.; Ali, M. U.; Peng, W. X.; Zhang, S. J.; Li, D. Z.; Zou, T. Y.; Li, Y. Y.; Jiao, S. B.; Chen, S. J. et al. Inkjet printed uniform quantum dots as color conversion layers for full-color OLED displays. *Nanoscale* **2020**, *12*, 2103–2110.

[3] Huang, Y. G.; Hsiang, E. L.; Deng, M. Y.; Wu, S. T. Mini-LED, micro-LED and OLED displays: Present status and future perspectives. *Light. Sci. Appl.* **2020**, *9*, 105.

[4] Liu, Z. J.; Lin, C. H.; Hyun, B. R.; Sher, C. W.; Lv, Z. J.; Luo, B. Q.; Jiang, F. L.; Wu, T.; Ho, C. H.; Kuo, H. C. et al. Micro-light-emitting diodes with quantum dots in display technology. *Light. Sci. Appl.* **2020**, *9*, 83.

[5] Dey, A.; Ye, J. Z.; De, A.; Debroye, E.; Ha, S. K.; Bladt, E.; Kshirsagar, A. S.; Wang, Z. Y.; Yin, J.; Wang, Y. et al. State of the art and prospects for halide perovskite nanocrystals. *ACS Nano* **2021**, *15*, 10775–10981.

[6] Zhang, F.; Zhong, H. Z.; Chen, C.; Wu, X. G.; Hu, X. M.; Huang, H. L.; Han, J. B.; Zou, B. S.; Dong, Y. P. Brightly luminescent and color-tunable colloidal $CH_3NH_3PbX_3$ (X = Br, I, Cl) quantum dots: Potential alternatives for display technology. *ACS Nano* **2015**, *9*, 4533–4542.

[7] Protesescu, L.; Yakunin, S.; Bodnarchuk, M. I.; Krieg, F.; Caputo, R.; Hendon, C. H.; Yang, R. X.; Walsh, A.; Kovalenko, M. V. Nanocrystals of cesium lead halide perovskites ($CsPbX_3$, X = Cl, Br, and I): Novel optoelectronic materials showing bright emission with wide color gamut. *Nano Lett.* **2015**, *15*, 3692–3696.

[8] Maes, J.; Balcaen, L.; Drijvers, E.; Zhao, Q.; De Roo, J.; Vantomme, A.; Vanhaecke, F.; Geiregat, P.; Hens, Z. Light absorption coefficient of $CsPbBr_3$ perovskite nanocrystals. *J. Phys. Chem. Lett.* **2018**, *9*, 3093–3097.

[9] Yang, H. J.; Cai, T.; Liu E. X.; Hill-Kimball K.; Gao J. B.; Chen O. Synthesis and transformation of zero-dimensional Cs_3BiX_6 (X = Cl, Br) perovskite-analogue nanocrystals. *Nano Res.* **2020**, *13*, 282–291.

[10] Duan, M.; Feng, Z. Y.; Wu, Y. W.; Yin, Y. M.; Hu, Z. P.; Peng, W. X.; Li, D. Z.; Chen, S. J.; Lee, C. Y.; Lien, A. Inkjet-printed micrometer-thick patterned perovskite quantum dot films for efficient blue-to-green photoconversion. *Adv. Mater. Technol.* **2019**, *4*, 1900779.
[11] Yin, Y. M.; Hu, Z. P.; Ali, M. U.; Duan, M.; Gao, L.; Liu, M.; Peng, W. X.; Geng, J.; Pan, S.; Wu, Y. W. et al. Full-color micro-LED display with $CsPbBr_3$ perovskite and CdSe quantum dots as color conversion layers. *Adv. Mater. Technol.* **2020**, *5*, 2000251.
[12] Chen, E. G.; Lin, J. Y.; Yang, T.; Chen, Y.; Zhang, X.; Ye, Y.; Sun, J.; Yan, Q.; Guo, T. L. Asymmetric quantum-dot pixelation for color-converted white balance. *ACS Photonics* **2021**, *8*, 2158–2165.
[13] Chen, M. J.; Yang, J.; Wang, Z. Y.; Xu, Z. Y.; Lee, H.; Lee, H.; Zhou, Z. W.; Feng, S. P.; Lee, S.; Pyo, J. et al. 3D nanoprinting of perovskites. *Adv. Mater.* **2019**, *31*, e1904073.
[14] Bae, J.; Lee, S.; Ahn, J.; Kim, J. H.; Wajahat, M.; Chang, W. S.; Yoon, S. Y.; Kim, J. T.; Seol, S. K.; Pyo, J. 3D-printed quantum dot nanopixels. *ACS Nano* **2020**, *14*, 10993–11001.
[15] Derby, B. Inkjet printing of functional and structural materials: Fluid property requirements, feature stability, and resolution. *Annu. Rev. Mater. Res.* **2010**, *40*, 395–414.
[16] De Gans, B. J.; Duineveld, P. C.; Schubert, U. S. Inkjet printing of polymers: State of the art and future developments. *Adv. Mater.* **2004**, *16*, 203–213.
[17] Tekin, E.; Smith, P. J.; Schubert, U. S. Inkjet printing as a deposition and patterning tool for polymers and inorganic particles. *Soft Matter* **2008**, *4*, 703–713.
[18] Xuan, T. T.; Shi, S. C.; Wang, L.; Kuo, H. C.; Xie, R. J. Inkjet-printed quantum dot color conversion films for high-resolution and full-color micro light-emitting diode displays. *J. Phys. Chem. Lett.* **2020**, *11*, 5184–5191.
[19] Li, H. G.; Duan, Y. Q.; Shao, Z. L.; Zhang, G. N.; Li, H. Y.; Huang, Y. A.; Yin, Z. P. High-resolution pixelated light emitting diodes based on electrohydrodynamic printing and coffee-ring-free quantum dot film. *Adv. Mater. Technol.* **2020**, *5*, 2000401.
[20] Gao, Y. Y.; Kang, C. B.; Prodanov, M. F.; Vashchenko, V. V.; Srivastava, A. K. Inkjet-printed, flexible full-color photoluminescence-type color filters for displays. *Adv. Eng. Mater.* **2022**, 2101553.
[21] Li, D. Y.; Wang, J. J.; Li, M. Z.; Xie, G. C.; Guo, B.; Mu, L.; Li, H. Y.; Wang, J.; Yip, H. L.; Peng, J. B. Inkjet printing matrix perovskite quantum dot light-emitting devices. *Adv. Mater. Technol.* **2020**, *5*, 2000099.
[22] Li, Y.; Chen, Z. W.; Liang, D.; Zang, J. Q.; Song, Z. H.; Cai, L.; Zou, Y. T.; Wang, X. C.; Wang, Y. S.; Li, P. D. et al. Coffee-stain-free perovskite film for efficient printed light-emitting diode. *Adv. Opt. Mater.* **2021**, *9*, 2100553.
[23] Li, H. G.; Duan, Y. Q.; Shao, Z. L.; Zhang, G. N.; Li, H. Y.; Huang, Y. A.; Yin, Z. P. High-resolution pixelated light emitting diodes based on electrohydrodynamic printing and coffee-ring-free quantum dot film. *Adv. Mater. Technol.* **2020**, *5*, 2000401.
[24] Shi, L. F.; Meng, L. H.; Jiang, F.; Ge, Y.; Li, F.; Wu, X. G.; Zhong, H. Z. In situ inkjet printing strategy for fabricating perovskite quantum dot patterns. Adv. Funct. *Mater.* **2019**, *29*, 1903648.
[25] Liu, Y.; Li, F. S.; Qiu, L. C.; Yang, K. Y.; Li, Q. Q.; Zheng, X.; Hu, H. L.; Guo, T. L.; Wu, C. X.; Kim, T. W. Fluorescent microarrays of *in situ* crystallized perovskite nanocomposites fabricated for patterned applications by using inkjet printing. *ACS Nano* **2019**, *13*, 2042–2049.
[26] Zhu, M. H.; Duan, Y. Q.; Liu, N.; Li, H. G.; Li, J. H.; Du, P. P.; Tan, Z. F.; Niu, G. D.; Gao, L.; Huang, Y. A. et al. Electrohydrodynamically printed high-resolution full-color hybrid perovskites. *Adv. Funct. Mater.* **2019**, *29*, 1903294.
[27] Shi, S. C.; Bai, W. H.; Xuan, T. T.; Zhou, T. L.; Dong, G. Y.; Xie, R. J. *In situ* inkjet printing patterned lead halide perovskite quantum dot color conversion films by using cheap and eco-friendly aqueous inks. *Small Methods* **2021**, *5*, 2000889.
[28] Zhou, Q. C.; Bai, Z. L.; Lu, W. G.; Wang, Y. T.; Zou, B. S.; Zhong, H. Z. *In situ* fabrication of halide perovskite nanocrystal-embedded polymer composite films with enhanced photoluminescence for display backlights. *Adv. Mater.* **2016**, *28*, 9163–9168.
[29] Huang, X. J.; Guo, Q. Y.; Yang, D. D.; Xiao, X. D.; Liu, X. F.; Xia, Z. G.; Fan, F. J.; Qiu, J. R.; Dong, G. P. Reversible 3D laser printing of perovskite quantum dots inside a transparent medium. *Nat. Photonics* **2020**, *14*, 82–88.
[30] Chen, X. M.; Zhang, F.; Ge, Y.; Shi, L. F.; Huang, S.; Tang, J. L.; Lv, Z.; Zhang, L.; Zou, B. S.; Zhong, H. Z. Centimeter-sized Cs_4PbBr_6 crystals with embedded $CsPbBr_3$ nanocrystals showing superior photoluminescence: Nonstoichiometry induced transformation and light-emitting applications. *Adv. Funct. Mater.* **2018**, *28*, 1706567.
[31] Meng, L. H.; Yang, C. G.; Meng, J. J.; Wang, Y. Z.; Ge, Y.; Shao, Z. Q.; Zhang, G. F.; Rogach, A. L.; Zhong, H. Z. *In-situ* fabricated anisotropic halide perovskite nanocrystals in polyvinylalcohol nanofibers: Shape tuning and polarized emission. *Nano Res.* **2019**, *12*, 1411–1416.
[32] Gao, A. J.; Yan, J.; Wang, Z. J.; Liu, P.; Wu, D.; Tang, X. B.; Fang, F.; Ding, S. H.; Li, X.; Sun, J. Y. et al. Printable $CsPbBr_3$ perovskite quantum dot ink for coffee ring-free fluorescent microarrays using inkjet printing. *Nanoscale* **2020**, *12*, 2569–2577.
[33] Jeon, S.; Lee, S. Y.; Kim, S. K.; Kim, W.; Park, T.; Bang, J.; Ahn, J.; Woo, H. K.; Chae, J. Y.; Paik, T. et al. All-solution processed multicolor patterning technique of perovskite nanocrystal for color pixel array and flexible optoelectronic devices. *Adv. Opt. Mater.* **2020**, *8*, 2000501.
[34] Yang, P. H.; Zhang, L.; Kang, D. J.; Strahl, R.; Kraus, T. High-resolution inkjet printing of quantum dot light-emitting microdiode arrays. *Adv. Opt. Mater.* **2020**, *8*, 1901429.
[35] Deegan, R. D.; Bakajin, O.; Dupont, T. F.; Huber, G.; Nagel, S. R.; Witten, T. A. Capillary flow as the cause of ring stains from dried liquid drops. *Nature* **1997**, *389*, 827–829.
[36] Sun, J. Z.; Bao, B.; He, M.; Zhou, H. H.; Song, Y. L. Recent advances in controlling the depositing morphologies of inkjet droplets. *ACS Appl. Mater. Interfaces* **2015**, *7*, 28086–28099.
[37] Yagci, Y.; Jockusch, S.; Turro, N. J. Photoinitiated polymerization: Advances, challenges, and opportunities. *Macromolecules* **2010**, *43*, 6245–6260.
[38] Farahani, R. D.; Dubé, M.; Therriault, D. Three-dimensional printing of multifunctional nanocomposites: Manufacturing techniques and applications. *Adv. Mater.* **2016**, *28*, 5794–5821.
[39] Corrigan, N.; Yeow, J.; Judzewitsch, P.; Xu, J. T.; Boyer, C. Seeing the light: Advancing materials chemistry through photopolymerization. *Angew. Chem., Int. Ed.* **2019**, *58*, 5170–5189.
[40] Tumbleston, J. R.; Shirvanyants, D.; Ermoshkin, N.; Janusziewicz, R.; Johnson, A. R.; Kelly, D.; Chen, K.; Pinschmidt, R.; Rolland, J. P.; Ermoshkin, A. et al. Continuous liquid interface production of 3D objects. *Science* **2015**, *347*, 1349–1352.
[41] Elliott, A. M.; Ivanova, O. S.; Williams, C. B.; Campbell, T. A. Inkjet printing of quantum dots in photopolymer for use in additive manufacturing of nanocomposites. *Adv. Eng. Mater.* **2013**, *15*, 903–907.
[42] Smith, M. J.; Malak, S. T.; Jung, J.; Yoon, Y. J.; Lin, C. H.; Kim, S.; Lee, K. M.; Ma, R. L.; White, T. J.; Bunning, T. J. et al. Robust, uniform, and highly emissive quantum dot-polymer films and patterns using thiol-ene chemistry. *ACS Appl. Mater. Interfaces* **2017**, *9*, 17435–17448.
[43] Hyun, B. R.; Sher, C. W.; Chang, Y. W.; Lin, Y. H.; Liu, Z. J.; Kuo, H. C. Dual role of quantum dots as color conversion layer and suppression of input light for full-color micro-LED displays. *J. Phys. Chem. Lett.* **2021**, *12*, 6946–6954.
[44] Li, H. G.; Liu, N.; Shao, Z. L.; Li, H. Y.; Xiao, L.; Bian, J.; Li, J. H.; Tan, Z. F.; Zhu, M. H.; Duan, Y. Q. et al. Coffee ring elimination and crystalline control of electrohydrodynamically printed high-viscosity perovskites. *J. Mater. Chem. C* **2019**, *7*, 14867–14873.
[45] Jia S. Q.; Li, G. Y.; Liu, P.; Cai, R.; Tang, H. D.; Xu, B.; Wang, Z. J.; Wu, Z. H.; Wang, K.; Sun, X. W. Highly luminescent and stable green quasi-2D perovskite-embedded polymer sheets by inkjet printing. *Adv. Funct. Mater.* **2020**, *30*, 1910817.
[46] Liang S.; Zhang, M. Y.; Biesold, G. M.; Choi, W.; He, Y. J.; Li, Z. L.; Shen, D. F.; Lin, Z. Q. Recent advances in synthesis, properties, and applications of metal halide perovskite nanocrystals/polymer nanocomposites. *Adv. Mater.* **2021**, *33*, 2005888.
[47] Hou, J.; Zhang, H. C.; Su, B.; Li, M. Z.; Yang, Q.; Jiang, L.; Song, Y. L. Four-dimensional screening anti-counterfeiting pattern by inkjet printed photonic crystals. *Chem. Asian J.* **2016**, *11*, 2680–2685.
[48] Shanahan, M. E. R.; Carré, A. Anomalous spreading of liquid drops on an elastomeric surface. *Langmuir* **1994**, *10*, 1647–1649.